EVAPORATION OF BINARY SOLUTIONS INTO DRY AIR ON A VERTICAL FLAT PLATE

HITOSHI KOSUGE, TSUTOMU ISHIKAWA, SHINICHI TANAKA AND KOICHI ASANO

Tokyo Institute of Technology, Tokyo, 152

Key Words: Evaporation, Heat Transfer, Mass Transfer, Diffusion Interaction, Ternary System, Vertical Flat Plate, Laminar Boundary Layer, Methanol 2-Propanol Air, Methanol Water Air

Experimental approaches were taken to examine heat and mass transfer in evaporation of the methanol–2-propanol and the methanol–water systems into dry air by a cocurrent vertical flat-plate wetted-wall column over wide ranges of gas and liquid flow rates and liquid concentrations.

The observed gas-phase sensible heat fluxes are compared with a theoretical analysis of heat transfer in a laminar boundary layer under high mass flux with finite tangential surface velocity. The effect of evaporative mass injection, tangential surface velocity and interactions between diffusion fluxes on the observed gas-phase diffusion fluxes are discussed. The observed diffusion fluxes are compared with a theoretical analysis of ternary mass transfer in a laminar boundary layer by taking into account the effect of interactions between diffusion fluxes under high mass flux with finite tangential surface velocity.

Introduction

Evaporation of volatile liquid mixtures into dry air under forced convection flow is a very complicated phenomenon, in which interactions between diffusion fluxes take place through the concentration driving forces of different species and mass fluxes affect the profiles of velocity, temperature and concentration near the interface. Although some theoretical and experimental approaches[11,13,15,18] have been taken to multicomponent mass transfer, few are known that take into account the effect of interactions between diffusion fluxes in the flow field.[11,15]

In our previous paper,[8] a numerical approach to ternary mass transfer in a laminar boundary layer was taken by considering the effect of interactions between diffusion fluxes with surface mass injection or suction. The purpose of the present work is to take an experimental approach to heat and mass transfer in evaporation of binary solutions into dry air for wide ranges of gas and liquid flow rates and liquid concentrations, and to compare them with the theoretical results proposed in our previous paper.[8] **Table 1** summarizes the theoretical results for heat and mass fluxes in a laminar boundary layer.[8]

1. Experimental Apparatus and Procedures

1.1 Experimental apparatus

Figure 1 shows a schematic diagram of the experimental apparatus. The evaporator was a cocurrent vertical flat-plate wetted-wall column, of which the test section was a brass rectangular duct of 30 × 30 mm in cross section with a 20 mm-wide, 100 mm-long gas-liquid contacting area. The upper edge of the wetted-wall was 25 mm from the lower edge of the convergent nozzle. On the opposite side of the wetted wall, a yoke-type 25 μm-outer diameter Chromel–Alumel thermocouple, 74 mm from the lower edge of the nozzle, was mounted on a traversing mechanism for measurements of gas-phase temperature profiles. On the reverse side of the wetted wall, a flow of

Table 1. Flux equations by laminar boundary layer theory

Sensible heat flux

$$Nu_x = 0.332 \cdot Pr^{1/3} \cdot Re_x^{1/2} \cdot g(B_H) \cdot h_H(F'(0), Pr) \quad (1)$$

$$g(B_H) = \frac{1}{0.0712 + 0.9288(1+B_H)^{0.8352}} \quad (2)^*$$

$$h_H(F'(0), Pr) = \{1 + 1.887F'(0)\}^{1/2} Pr^{\sqrt{F'(0)}/6} \quad (3)^{17)*}$$

$$B_H = Re_x \cdot Pr \cdot (v_s/U_\infty)/Nu_x \quad (4)$$

Diffusion flux

$$Sh_{ix}(J_{ix}/N_{ix}) = Sh_{ix}^0(J_{ix}^0/N_{ix}^0) \cdot G_i \cdot P_i = 0.332 \cdot Sc_{ii}^{1/3} \cdot Re_x^{1/2} \cdot G_i \cdot P_i \quad (i=A, B) \quad (5)$$

$$P_i = 1 + 0.64\left(\frac{Sc_{ii}^{0.86} Sc_{jj}^{0.19}}{Sc_{ij}} \frac{\Delta\omega_j}{\Delta\omega_i}\right) \quad \begin{matrix}(i,j=A,B)\\(i \neq j)\end{matrix} \quad (6)$$

$$G_i = J_{ix}/J_{ix}(F(0)=0,\ F'(0)=0) \quad (i=A, B) \quad (7)$$

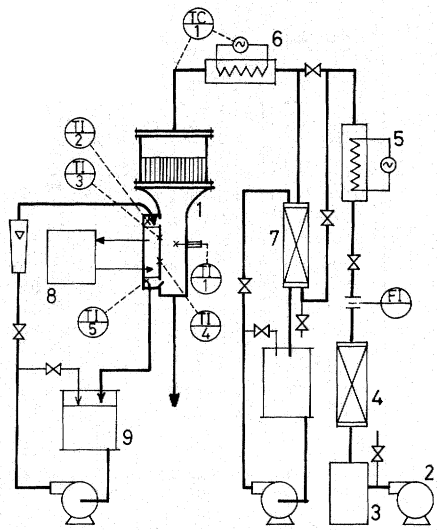
$$F(0) = -2(v_s/U_\infty)Re_x^{1/2} \quad (8)$$

$$F'(0) = u_s/U_\infty \quad (9)$$

$$Sc_{ij} = \mu/\rho D_{ij} \quad (i,j=A, B) \quad (10)$$

* These correlations were obtained from the numerical data with the condition of $1 < B_H < 10$, $0 < F'(0) < 1$, $0.01 < Pr < 1000$ by the quasi-linearization method.[8]

Received May 12, 1988. Correspondence concerning this article should be addressed to H. Kosuge.



1 Test section
2 Blower
3 Dehumidifier
4 Silica gel dehumidifier
5,6 Heater
7 Saturator
8 Constant-temperature bath
9 Reservoir
TI Thermocouple
FI Orifice flow meter

Fig. 1. Schematic diagram of experimental apparatus

constant-temperature water was arranged to control the evaporation rates of the liquid. On the side walls of the test section, two view windows were attached for observation of the falling liquid film.

Air was supplied to the test section by a blower through a silica gel-packed dehumidifier, temperature controllers and a convergent nozzle with 5 mm-outer diameter brass tube calming grids.

Preliminary measurements of the velocity and temperature profiles in the test section for cooling of air and evaporation of the pure liquids (methanol, 2-propanol and water) into dry air showed good agreement with the theoretical values for a laminar boundary layer.

1.2 Measurements

1) Liquid flow rates and concentrations: The flow rates of the evaporating liquids were measured by a rotameter with an accuracy of better than 1%. The liquid concentrations were measured by a precision refractometer with an accuracy of better than 0.1 mol%.

2) Gas flow rates and concentrations: The flow rates of the air were measured by a calibrated orifice flow meter. The bottom and top concentrations of the gases were measured by a gas chromatograph with an accuracy of better than 0.5 mol%.

3) Mass and diffusion fluxes: The gas-phase average mass fluxes of volatile components, N_A, N_B, were determined from the gas flow rates and the bottom and top gas concentrations. The gas-phase average diffusion fluxes of the volatile components, J_{As}, J_{Bs}, were obtained by the following equations:[9,10]*

$$J_{is}=N_i-(N_A+N_B)\omega_{is} \quad (i=A,\ B) \tag{11}$$

The gas-phase average diffusion fluxes were made dimensionless by:[8,10]

$$Sh_{Gi}(J_{is}/N_i)=J_{is}Z/\rho_{Gs}D_{Gii}\Delta\omega_{Gi} \quad (i=A,\ B) \tag{12}$$

where D_{Gii} were multicomponent diffusion coefficients defined by:[12]

$$D_{Gii}=\mathscr{D}_{GiC}(y_i\mathscr{D}_{GjC}+(1-y_i)\mathscr{D}_{Gij})/S \tag{13a}$$

$$D_{Gij}=y_i\mathscr{D}_{GjC}(\mathscr{D}_{GiC}-\mathscr{D}_{Gij})/S \tag{13b}$$

$$S=y_A\mathscr{D}_{GBC}+y_B\mathscr{D}_{GAC}+y_C\mathscr{D}_{GAB} \quad (i,j=A,\ B) \tag{13c}$$

4) Surface velocities at the liquid film: The normal components of the surface velocities at the gas-liquid interface were obtained from the observed mass fluxes.[9] The tangential components of the surface velocities were calculated by assuming parabolic velocity profiles in a falling liquid film.[3,16]

5) Surface temperatures and concentrations: The surface temperatures of the liquid film, T_{sob}, were estimated from the observed temperature profiles by an extrapolation method. The surface concentrations of the liquid film were evaluated from the liquid bulk concentrations by use of Higbie's model,[16] as was the case for the binary distillation[7] and condensation of mixed vapors.[2] The gas-phase surface concentrations were evaluated from the saturated vapor pressures of the pure components at the surface temperatures.

6) Gas-phase sensible heat fluxes: The gas-phase local sensible heat fluxes, q_{Gx}, were obtained from the observed temperature gradients, from which the gas-phase local Nusselt numbers were evaluated.[7,10]

1.3 Physical properties

The vapor pressures of the pure liquids were calculated from Antoine's equation. The binary diffusion coefficients and the viscosities of the pure components were estimated by Hirschfelder's method[14] and the thermal conductivities of the pure components by Eucken's method.[14] The viscosities and the thermal conductivities of mixed gases were estimated by Wilke's method.[14]

1.4 Ranges of variables

Evaporation runs were made for the methanol-2-propanol-air and the methanol–water–air systems under cocurrent flow conditions at atmospheric pressure for wide ranges of liquid and gas flow rates and

* The mass and diffusion fluxes for air, N_C and J_{Cs}, are not considered in the later sections because of the following relationships[1]:

$$N_C=0 \tag{A1}$$

$$J_{Cs}=-(J_{As}+J_{Bs}) \tag{A2}$$

Table 2. Ranges of variables

System		methanol–2-propanol–air	methanol–water–air
x_A	[—]	0.30–0.76	0.18–0.77
Γ	[kg/(m·s)]	0.008–0.053	0.012–0.063
Re_G	[—]	3100–18300	3600–14000
Pr_{Gs}	[—]	0.74–0.86	0.73–0.78
Sc_{GAA}	[—]	0.62–0.93	0.71–0.91
Sc_{GAB}	[—]	1.70–65.6	32.0–96.0
Sc_{GBB}	[—]	0.81–1.40	0.61–0.68
Sc_{GBA}	[—]	5.70–102	9.60–110
$\Delta\omega_{GA}$	[—]	0.016–0.513	0.177–0.514
$\Delta\omega_{GB}$	[—]	0.036–0.432	0.015–0.125
$\overline{F(0)}$	[—]	−0.08–−0.98	−0.16–−0.72
$F'(0)$	[—]	0.04–0.62	0.21–0.43
B_H	[—]	0.09–1.56	0.18–1.10

liquid concentrations. **Table 2** shows the ranges of variables for the present study.

2. Experimental Results

2.1 Gas-phase temperature profiles and sensible heat fluxes

Figure 2 shows an example of the observed gas-phase temperature profiles for the methanol–2-propanol–air system. The ordinate of the figure is the dimensionless temperatures and the abscissa the dimensionless distance from the gas-liquid interface corrected for the effect of the entry length, x_0, by Eckert's method.[5] The solid lines in the figure represent the theoretical profiles for the operating conditions calculated by laminar boundary layer theory with surface mass injection, where B_H, the transfer number for heat transfer,** represents a measure of evaporative mass injection.[4,6] A regular decrease in thickness of the thermal boundary layer with increase of B_H was observed. The data showed good agreement with the theoretical profiles.

Figure 3 shows the effect of B_H on the observed gas-phase local sensible heat fluxes for the methanol–2-propanol–air system. The ordinate is the local Nusselt numbers corrected for the effect of tangential surface velocity by Eq. (3). The solid line in the figure represents the theoretical values for low mass flux conditions ($B_H=0$) and the dotted lines are the theoretical ones under high mass flux conditions by laminar boundary layer theory. A systematic decrease in the sensible heat fluxes with increase of B_H was observed.

Figure 4 shows a correlation for the gas-phase local Nusselt numbers in terms of gas-phase local Reynolds numbers, where $g(B_H)$ in the ordinate represents the effect of evaporative mass injection on the local

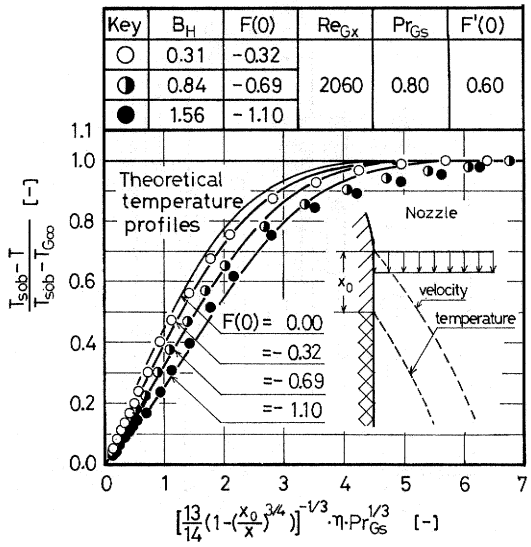


Fig. 2. An example of observed gas-phase temperature profiles for the methanol–2-propanol–air system

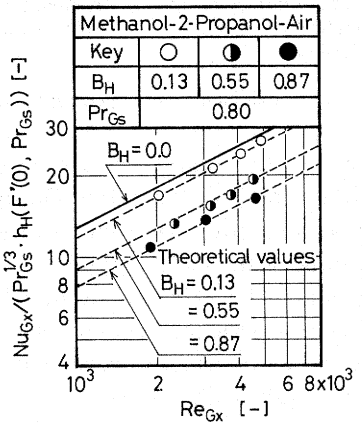


Fig. 3. Effect of evaporative mass injection on gas-phase local sensible heat fluxes

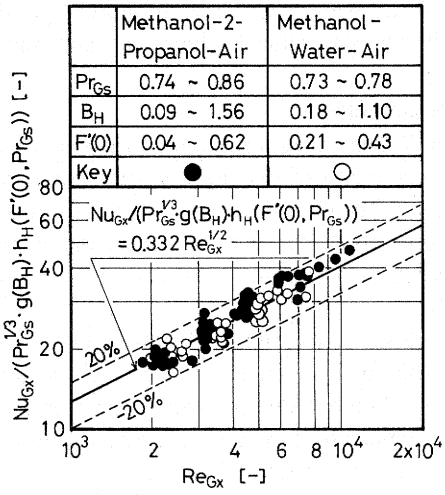


Fig. 4. Gas-phase local sensible heat fluxes for evaporation of binary mixtures into air

Nusselt numbers by Eq. (2). The solid line in the figure represents the low mass flux correlation by Eq. (1). All the data for the methanol–2-propanol–air and

** Relationship between B_H and $F(0)$ is given by[1]:

$$F(0)=-(2B_H/Pr)\theta_T'(0) \qquad \text{(A3)}$$

where $\theta_T'(0)$ is the dimensionless temperature gradient at the gas-liquid interface.

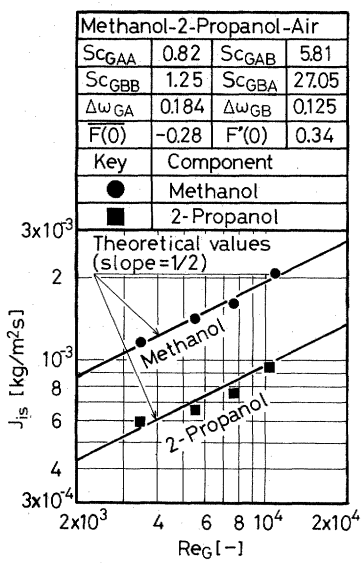


Fig. 5. Effect of Reynolds number on diffusion fluxes

the methanol–water–air systems showed good agreement with the theory.

2.2 Gas-phase diffusion fluxes

Figure 5 shows the effect of gas-phase average Reynolds number on the gas-phase average diffusion fluxes of the methanol and 2-propanol for the methanol–2-propanol–air system. The solid lines in the figure represent the theoretical values by laminar boundary layer theory.[8] The observed diffusion fluxes showed good agreement with the theory. Similar results were also obtained for the other runs.

Figure 6 shows the effect of evaporative mass injection on the average diffusion fluxes of the methanol and 2-propanol for the methanol–2-propanol–air system. The abscissa is the average stream function at the interface.[7] The solid lines in the figure represent the theoretical values.[8] Again, good agreement between the data and theory was observed. **Figure 7** shows the effect of tangential surface velocity on the diffusion fluxes of the methanol and 2-propanol. The solid lines in the figure represent the theoretical values by laminar boundary layer theory. The data showed good agreement with the theory.

3. Ternary Diffusion Fluxes

3.1 Effect of interactions between diffusion fluxes

Figure 8 shows the effect of driving force ratio on the diffusion fluxes of the methanol and 2-propanol for the methanol–2-propanol–air system. G_i in the ordinate, defined by Eq. (7), represents the effect of high mass flux with finite tangential surface velocity on the diffusion fluxes. The two solid lines in the figure represent the theoretical diffusion fluxes of the methanol and 2-propanol calculated by the method proposed in our previous paper.[8] Although some scattering was observed for the data for 2-propanol, fairly good agreement between the data and the

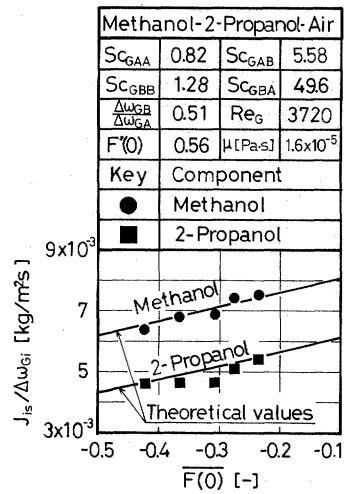


Fig. 6. Effect of evaporative mass injection on diffusion fluxes

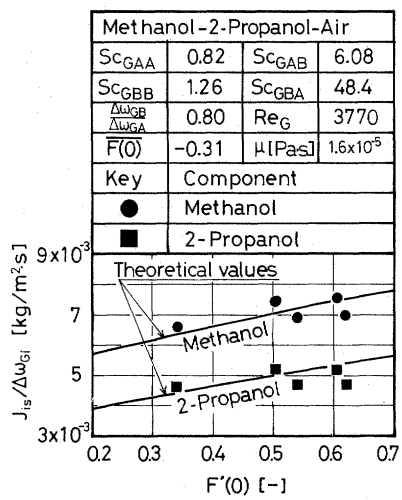


Fig. 7. Effect of tangential surface velocity on diffusion fluxes

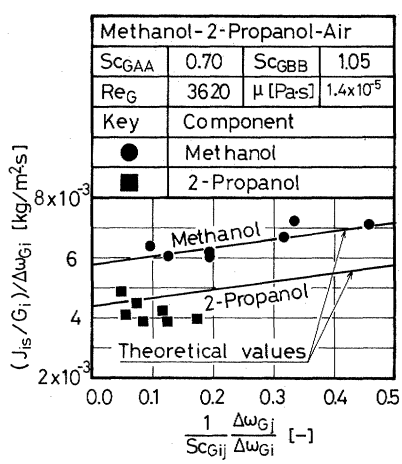


Fig. 8. Effect of driving force ratio on diffusion fluxes

theory was observed. This may indicate a possibility of the effect of interactions between diffusion fluxes for this system.

To illustrate this point in more detail, the dimen-

sionless diffusion fluxes of the methanol and 2-propanol corrected for the effect of high mass flux with finite tangential surface velocity at nearly constant P_i values are plotted against Reynolds number in **Fig. 9**, where P_i is a measure for the effect of interactions between diffusion fluxes by Eq. (6). The solid line in the figure represents the low mass flux correlation for binary mass transfer given by:

$$Sh^0_{Gi}(J^0_{is}/N^0_i)=\int_0^z (1/x)Sh^0_{Gix}(J^0_{ix}/N^0_{ix})dx$$
$$=0.664\cdot Re_G^{1/2}\cdot Sc_{Gii}^{1/3} \qquad (i=A, B) \quad (14)$$

The two dotted lines are the theoretical values for $P_i=1.23$ (methanol) and 1.06 (2-propanol), respectively. Good agreement between the data and the theory was observed.

3.2 Correlation for diffusion fluxes in ternary mass transfer

Figure 10 shows a final correlation for the observed diffusion fluxes in the ternary system. The ordinate is the dimensionless diffusion fluxes corrected for the effect of high mass flux with finite tangential surface velocity by use of G_i and for the effect of interactions between diffusion fluxes by Eq. (6). The solid line in the figure represents the correlation for the theoretical data of the average diffusion fluxes in the ternary system under high mass flux with finite tangential surface velocity given by:

$$Sh_{Gi}(J_{is}/N_i)=0.664\cdot Re_G^{1/2}\cdot Sc_{Gii}^{1/3}\cdot G_i\cdot P_i$$
$$(i=A, B) \qquad (15)$$

All the diffusion fluxes for the methanol–2-propanol–air and the methanol–water–air systems showed good agreement with the theoretical correlation, as was the case for ternary distillation.[10]

For comparison, the dimensionless diffusion fluxes without correction for the effect of high mass flux, tangential surface velocity and interaction between diffusion fluxes are plotted against Reynolds number in **Fig. 11**. A large scattering of the data was observed, as was expected.***,****

*** Maximum deviations from Eq. (15) for the diffusion fluxes with the following corrections are:

Diffusion flux	Maximum deviation
$Sh_{Gi}(J_{is}/N_i)/(Sc_{Gii}^{1/3}\cdot G_i\cdot P_i)$	24%
$Sh_{Gi}(J_{is}/N_i)/(Sc_{Gii}^{1/3}\cdot G_i)$	34%
$Sh_{Gi}(J_{is}/N_i)/(Sc_{Gii}^{1/3})$	60%

**** The conditions under which the effect of high mass flux, tangential surface velocity and interaction between diffusion fluxes on the diffusion fluxes may show more than 10% deviations are given respectively by use of these numerical correlations:

$$|F(0)|>0.15$$
$$F'(0)>0.15$$
$$(Sc_{ii}^{0.86}Sc_{jj}^{0.19}/Sc_{ij})(\Delta\omega_j/\Delta\omega_i)>0.16$$

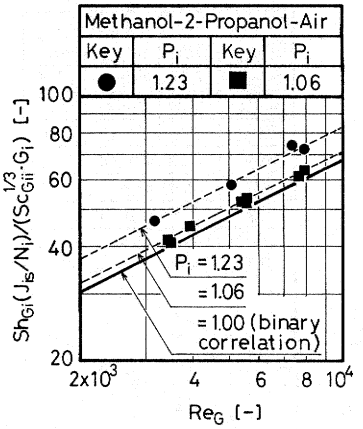


Fig. 9. Effect of interaction between diffusion fluxes

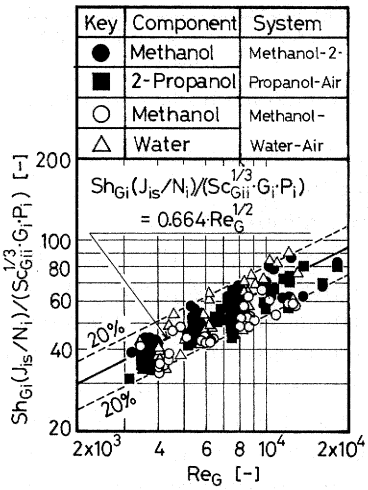


Fig. 10. Final correlation for diffusion fluxes in ternary mass transfer

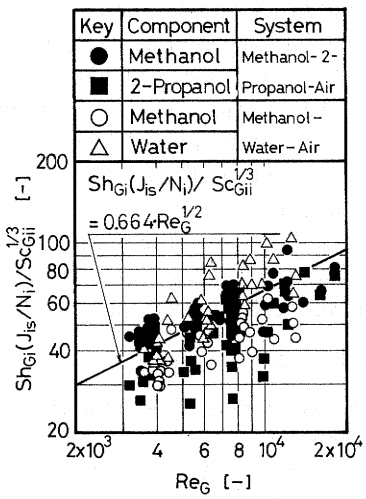


Fig. 11. Comparison of observed diffusion fluxes with theoretical ones for binary mass transfer under low mass flux conditions

Conclusions

Experimental approaches to the examination of heat and mass transfer in evaporation of the methanol–2-propanol and the methanol–water sys-

tems into dry air by a cocurrent vertical flat plate wetted-wall column were taken, leading to the following conclusions.

1) The observed sensible heat fluxes corrected for the effect of high mass flux with finite tangential surface velocity were in good agreement with the laminar boundary layer theory.

2) The effect of high mass flux, tangential surface velocity and interactions between diffusion fluxes on the observed diffusion fluxes showed good agreement with the laminar boundary layer theory for the ternary system.

3) The observed diffusion fluxes corrected for the effect of high mass flux with finite tangential surface velocity and of interactions between diffusion fluxes also showed good agreement with the theory.

Nomenclature

B_H	=	transfer number for heat transfer defined by Eq. (4) ($=Re_x Pr(v_s/U_\infty)/Nu_x$)	[—]
c_p	=	specific heat at constant pressure	[J/(kg·K)]
$\mathscr{D}_{ij}$	=	binary diffusion coefficient	[m²/s]
D_{ij}	=	multicomponent diffusion coefficient for i–j pair	[m²/s]
F	=	dimensionless stream function ($=\psi/(vxU_\infty)^{1/2}$)	[—]
$\overline{F(0)}$	=	average dimensionless stream function $\left(=(1/Z)\int_0^Z F(0)dx=-(4/3)(v_s/U_\infty)Re_G^{1/2}\right)$	[—]
G_i	=	function defined by Eq. (7)	[—]
$g_H(B_H)$	=	function defined by Eq. (2)	[—]
h_H	=	function defined by Eq. (3)	[—]
J_i	=	diffusion flux for the i-th component	[kg/(m²·s)]
N_i	=	mass flux for the i-th component	[kg/(m²·s)]
Nu_x	=	local Nusselt number ($=q_x x/\kappa(T_s-T_\infty)$)	[—]
P_i	=	function defined by Eq. (6)	[—]
Pr	=	Prandtl number ($=c_p\mu/\kappa$)	[—]
q_x	=	local sensible heat flux	[W/m²]
Re	=	Reynolds number ($=\rho U_\infty Z/\mu$)	[—]
Re_x	=	local Reynolds number ($=\rho U_\infty x/\mu$)	[—]
S	=	parameter defined by Eq. (13c)	[m²/s]
Sc_{ij}	=	multicomponent Schmidt number with multicomponent diffusion coefficient ($=\mu/\rho D_{ij}$)	[—]
Sh_i	=	multicomponent Sherwood number with multicomponent diffusion coefficient ($=N_i Z/\rho D_{ii}\Delta\omega_i$)	[—]
T	=	temperature	[K]
u_s	=	tangential surface velocity	[m/s]
U_∞	=	free stream velocity	[m/s]
v_s	=	normal component of interfacial velocity	[m/s]
x	=	distance from lower edge of nozzle	[m]
x_i	=	liquid-phase mole fraction	[—]
x_0	=	distance between lower edge of nozzle and upper edge of wetted wall	[m]
y	=	distance from the liquid film	[m]
y_i	=	gas-phase mole fraction	[—]
Z	=	length of wetted wall	[m]
Γ	=	liquid mass flow rate per unit perimeter	[kg/(m·s)]
$\Delta\omega_i$	=	concentration driving force for the i-th component	[—]
η	=	dimensionless distance ($=(y/x)Re_x^{1/2}$)	[—]
$\theta'_T(0)$	=	dimensionless temperature gradient at the interface	[—]
κ	=	thermal conductivity	[W/(m·s·K)]
μ	=	viscosity	[Pa·s]
ν	=	kinematic viscosity	[m²/s]
ρ	=	density	[kg/m³]
ψ	=	stream function	[m²/s]
ω_i	=	mass fraction for the i-th component	[—]

〈Subscript〉

A	=	more volatile component
B	=	less volatile component
C	=	inert gas (air)
G	=	gas-phase
ob	=	observed value
s	=	interface
∞	=	free stream

Literature Cited

1) Asano, K.: "Busshitsu Idoron", pp. 10, 59, Kyoritsu Shuppan, Tokyo (1976).
2) Asano, K. and S. Matsuda: *Kagaku Kogaku Ronbunshu*, **8**, 317 (1982).
3) Bird, R. B., W. E. Stewart and E. N. Lightfoot: "Transport Phenomena", p. 39, John Wiley & Sons, New York (1960).
4) Chuchottaworn, P., A. Fujinami and K. Asano: *J. Chem. Eng. Japan*, **17**, 1 (1984).
5) Eckert, E. R. G. and R. M. Drake, Jr.: "Heat and Mass Transfer", p. 173, McGraw-Hill, New York (1959).
6) Hoffman, T. W. and L. L. Ross: *Int. J. Heat Mass Transfer*, **15**, 599 (1972).
7) Ito, A. and K. Asano: *Chem. Eng. Sci.*, **37**, 1007 (1982).
8) Kosuge, H., T. Ishikawa and K. Asano: *J. Chem. Eng. Japan*, **20**, 525 (1987).
9) Kosuge, H., T. Johkoh and K. Asano: *Chem. Eng. Commun.*, **34**, 111 (1985).
10) Kosuge, H., Y. Mochizuki and K. Asano: *J. Chem. Eng. Japan*, **21**, 645 (1988).
11) Krishna, R.: *Trans. Inst. Chem. Eng.*, **59**, 35 (1981).
12) Krishna, R. and G. L. Standart: *Chem. Eng. Commun.*, **3**, 201 (1979).
13) Krishnamurthy, R. and R. Taylor: *Chem. Eng. J.*, **25**, 47 (1982).
14) Reid, R. C., J. M. Prausnitz and T. K. Sherwood: "The Properties of Gases and Liquids", 3rd Ed., pp. 394, 473, 549, McGraw-Hill, New York (1975).
15) Sato, T., T. Yonemoto and T. Tadaki: *Kagaku Kogaku Ronbunshu*, **9**, 509 (1983).
16) Sherwood, T. K., R. L. Pigford and C. R. Wilke: "Mass Transfer", pp. 78, 206, McGraw-Hill, New York (1975).
17) Shirotsuka, T. and A. Hirata: *Kagaku Kōgaku*, **35**, 78 (1971).
18) Taitel, Y. and A. Tamir: *Int. J. Heat Mass Transfer*, **18**, 123 (1975).